Determination of absorption coefficient by digital holographic measurement of optical excitation

David C. Clark* and Myung K. Kim

Digital Holography and Microscopy Laboratory, Department of Physics, University of South Florida, 4202 East Fowler Avenue, Tampa, Florida 33620, USA

*Corresponding author: dcclark@mail.usf.edu

Received 22 December 2010; revised 16 February 2011; accepted 18 February 2011; posted 23 February 2011 (Doc. ID 140049); published 13 April 2011

Digital holographic microscopy produces quantitative phase analysis of a specimen with excellent optical precision. In this study, this imaging method has been used to observe and measure induced thermal lensing by optical excitation. Previous studies have derived these phase shifts from intensity profiles for the determination of photothermal properties of very transparent materials. We have measured physical observables and determined the absorption coefficients of methanol and ethanol with improved precision and accuracy over traditional thermal lens spectroscopy methods. © 2011 Optical Society of America

OCIS codes: 090.0090, 090.1995, 350.6830.

1. Introduction

When a beam of incident light passes through a medium, that medium may absorb some of the energy of the beam. This absorbed energy, in turn, will cause a change in temperature of the absorbing region of the media which then will diffuse to other parts of the medium and its surroundings in some regular way described by the thermal properties of the media involved. Because the index of refraction is a temperature-dependent property, the temperature gradient also causes a refractive index gradient. This causes a change in the optical path length in these regions to the partially absorbed beam of light as well as any other beam of light incident on the affected area of the media. This effect is referred to as thermal lensing and has been the focus of many other studies as an indicator of the optical and thermal properties of materials [1,2].

Because of the change in optical path length, a resulting phase shift can be detected at a plane on the far side of the medium. Both a two-dimensional (2D) infinite and a three-dimensional (3D) finite model have been developed to associate this phase shift with the medium's absorption coefficient for a cw laser-induced mode-mismatched dual beam setup such as that used in the current study [3,4]. The 2D infinite model has the assumption, among others, that the sample thickness is large enough that axial heat flow and sample edge effects can be ignored. This method becomes inadequate for the study of thin-film samples. The 3D finite model is able to successfully describe samples of all thicknesses; however, it lacks the convenient mathematical relation to thermo-optical properties of the 2D infinite model. For ease and freedom of setup, it is wise to choose sample parameters that are compatible with the 2D model for studies involving such conclusions.

To maintain validity of the 2D infinite model, several assumptions are made and experimental design should take these into account. The sample cell thickness should be short compared to the confocal distance of the beams to ensure that the spot size remains relatively constant through the sample. The sample cell dimensions should be large compared with the excitation beam radius so that both radial and axial edge effects can be ignored. The sample should absorb very little power to avoid convection effects. Finally, the temperature coefficient of

0003-6935/11/121668-05$15.00/0

refractive index, $\frac{dn}{dT}$, should be constant in the range of temperatures observed. With these assumptions in mind, the laser induced change in temperature within the sample can be described by [3]

$$\Delta T(r,t) = \frac{2P\alpha}{\pi c\rho w^2}\int_0^t \frac{1}{1+2t'/\tau}\exp\left(-\frac{2r^2/w^2}{1+2t'/\tau}\right)\mathrm{d}t', \tag{1}$$

where r is the radial distance from the beam axis, t is the time of exposure to the excitation beam, P is the total excitation beam power at the sample, α, c, and ρ are the absorption coefficient, specific heat, and density of the sample, respectively, and w is the excitation beam radius in the sample. The characteristic thermal time constant, τ, is given by $\tau = \frac{w^2 c\rho}{4\kappa}$ with thermal conductivity, κ. The resulting refractive index gradient can be described by

$$n(r,t) = n_0 + \frac{dn}{dT}\Delta T(r,t), \tag{2}$$

where n_0 is the index of refraction at the starting temperature of the sample. This leads directly to phase shift described by

$$\begin{aligned}\phi &= \frac{2\pi}{\lambda} l[n(r,t) - n(0,t)] \\ &= \frac{2\pi}{\lambda} l\frac{dn}{dT}[\Delta T(r,t) - \Delta T(0,t)],\end{aligned} \tag{3}$$

where λ is the wavelength of the probe beam and l is the thickness of the sample. Substituting Eq. (1) into Eq. (3), the phase shift can be rewritten as

$$\phi = \theta\int_0^t \frac{1}{1+2t'/\tau}\left[1-\exp\left(-\frac{2r^2/w^2}{1+2t'/\tau}\right)\right]\frac{\mathrm{d}t'}{\tau}, \tag{4}$$

where

$$\theta = -\frac{Pal(dn/dT)}{\kappa\lambda}. \tag{5}$$

Previous experimental methods have been developed to approximate this phase shift and have been used to measure very low absorption coefficients of materials with good agreement to expected values [1,2]. These methods detect the intensity, with and without an induced thermal lens present in the media, through a pinhole at a distance several meters away from the sample. This difference in intensity is used, through further mathematical approximation and fitting, to determine the change in the wavefront of the incident beam and, therefore, the phase shift resulting from the thermal lens [1–5]. While this is a sensitive photothermal spectroscopy method [6], this is not a direct measure of the resultant phase shift and gives rise to additional error as discussed in [4].

Since digital holography is a phase-imaging method [7,8], this phase shift can be directly measured, without further approximations, in a process similar to photothermal interferometry [9]. In addition, there is no necessary minimum distance from the thermal lens to the detector plane when measuring by digital holography. It was the goal of our study to image the induced thermal lens directly and accurately and to use this compact, fast, and robust method to determine the absorption coefficients of transparent materials far below the detection level of standard spectrometers and with improved accuracy and precision over traditional photothermal spectroscopy methods.

2. Experimental Methods

Figure 1 shows a diagram of the experimental apparatus. A Mach–Zehnder interferometer is used to create the hologram of the sample using low-power (~2.5 mW) 633 nm laser light. The imaging beams (from a single source) are delivered by a 50:50 split fiber optic cable (reference/probe beams), which are then collimated and passed through polarizers upon entering the system. The polarizers can be adjusted to aid in beam level balancing. The two beams then pass through matched microscope objectives before being superposed with one another by the beam combiner, differing only in that the probe beam path includes the transparent sample as shown. The resulting hologram is recorded by a digital CCD camera placed atop the setup and passed into our LabVIEW personal computer platform for amplitude and phase reconstruction based on the angular spectrum method [10].

An integrated optical excitation arm delivers a high-powered 532 cw laser beam to the system via a fiber optic cable and collimation setup. The beam is then passed through a 10:1 focal length lens pair to create a much reduced collimated beam radius. A dichroic mirror reflects this excitation beam down toward the sample while allowing the probe beam to transmit up toward the CCD camera. The excitation

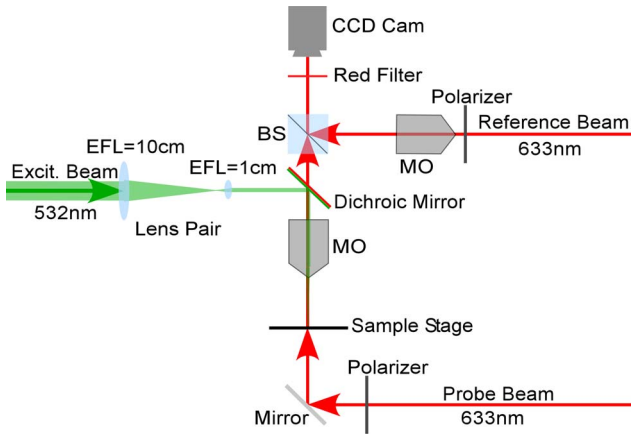

Fig. 1. (Color online) Experimental apparatus. The excitation beam (green) is focused downward through the sample by the probe-shared microscope objective (MO). The probe beam (red) is the object arm of the Mach–Zehnder interferometer and passes upward through the sample, combines with the reference beam, and creates the hologram captured by the CCD camera.

beam passes through the shared microscope objective that focuses the already thin beam through the sample area. The microscope objectives are chosen to have long effective focal lengths to aid in meeting the requirements of the 2D infinite model described above. A removable red filter is placed just in front of the CCD camera to filter any 532 excitation light leaking through the dichroic mirror. This "leaky" light, however, can be used to find the excitation beam radius and spot location as well as its waist along the beam axis by temporarily removing the red filter. The excitation beam radius, w, is defined as the radius at which our Gaussian beam amplitude reduces to e^{-2} of its maximum value. With the red filter in place, a hologram, containing complete phase and amplitude information, is captured by the CCD camera and processed by our software routines to reconstruct the phase image in real time both with and without excitation.

The sample consists of a pure liquid in a standard glass cuvette of cross-sectional area 5 mm by 10 mm, with a sealable lid. This sample is then placed on the sample stage on its side oriented with a 5 mm path length. While viewing the phase image, with the optical excitation beam on, the object stage was translated along the beam path (z direction) until the focus of the excitation beam was centered within the sample. At this position, a well-defined phase signal, i.e., the thermal lens, was clearly observed (Fig. 2). The faint diagonal fringing is a result of stray light interference within the setup. This can be removed through alternate construction options or additional software filtering; however, this was not necessary as the aberration did not affect our measurement goals at this time. A cross section through the center of this thermal lens was used to plot the profile of the phase shift as a function of radial distance from the z axis of the excitation beam (Fig. 3). It should be noted that,

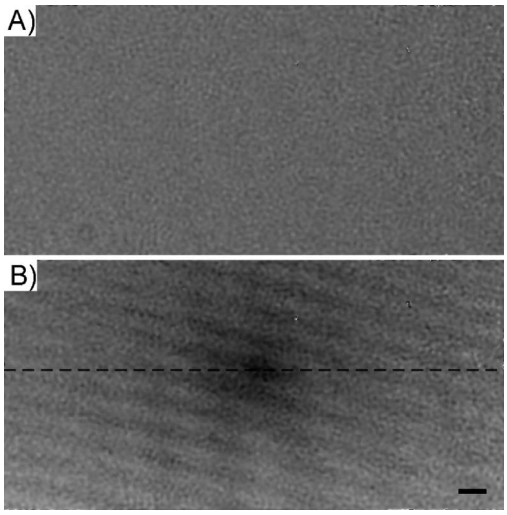

Fig. 2. Phase images of methanol with (A) no excitation beam and (B) 700mW excitation beam power. The phase scale of both images ranges from 0 (black) to 2π (white) and the spatial scale bar is 100 μm. The dashed line indicates the selected cross section used for further analysis.

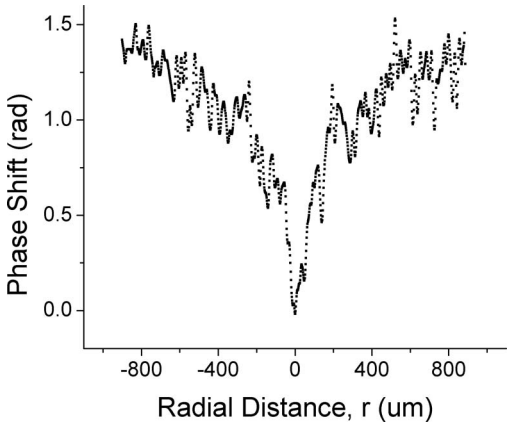

Fig. 3. Cross-sectional profile of the thermal lens shown in Fig. 2 (b) (dashed curve).

due to the time-sensitivity of the thermal effect, attention must be given to excitation beam exposure time to ensure that measurements are taken in the proper regime. All measurements for the purpose of determination of absorption coefficient, for example, were performed at exposure times greater than 2000τ to ensure steady-state regime was approached. Though the model is time-resolved and our previous work demonstrates excellent temporal agreement [11], near steady-state measurements drastically reduce error due to timing of measurements.

3. Results

The experimental parameters and determined absorption coefficients, α_{exp}, for methanol and ethanol are shown in Table 1. The measured phase shift at $t = 30$ s and $r = 900\,\mu$m under 700 mW excitation power was used to find the absorption coefficient that solved the 2D infinite model at this position and time. This determined absorption coefficient was then used to predict the entire phase profile of the thermal lens formed at varying excitation powers from 0–550 mW. Figure 4 shows the raw phase data for methanol and ethanol at several of these powers superposed on the predictions of the model with excellent fit. The displayed results are characteristic of the full range of powers tested. Note also that each plot of experimental data posted here has not been averaged, but is the result of a single hologram. If desired, higher phase resolution can be achieved by averaging repeated phase profiles in postprocess

Table 1. Experimental Parameters

	Methanol	Ethanol
w	43 μm	43 μm
l	5 mm	5 mm
dn/dT	-3.9×10^{-4} °C^{-1}	-4.0×10^{-4} °C^{-1}
κ	0.202 W/m/°C	0.167 W/m/°C
λ	633 nm	633 nm
P	0–550 mW	0–550 mW
τ	4.7 ms	5.7 ms
t	30 s	30 s
α_{exp}	3.6×10^{-4} cm^{-1}	2.4×10^{-4} cm^{-1}

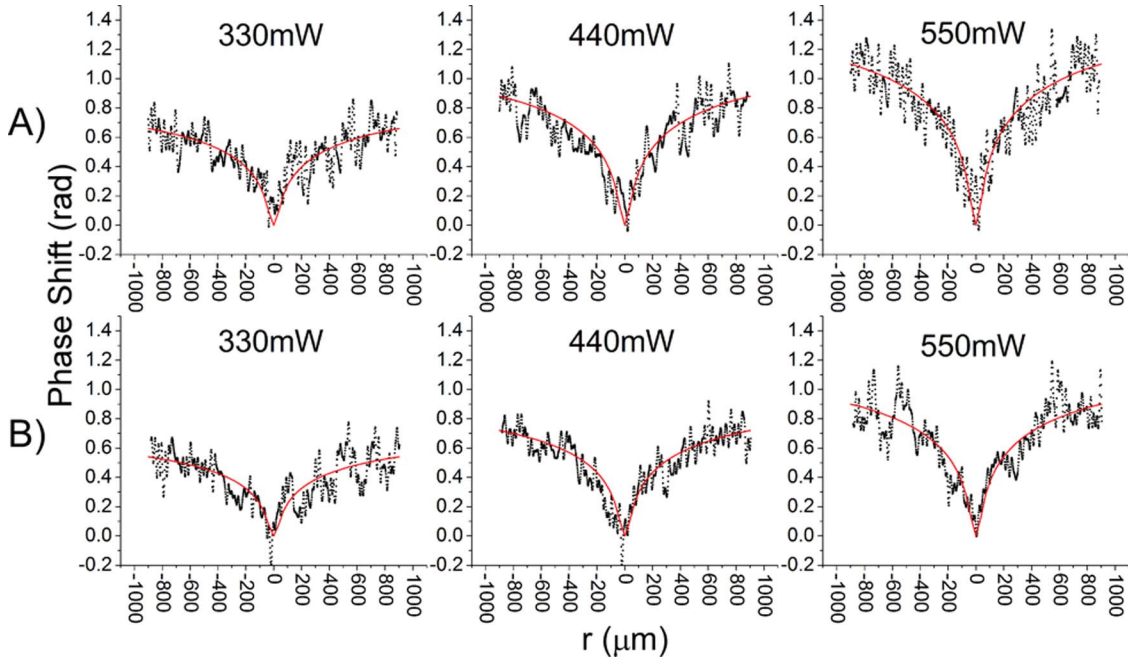

Fig. 4. (Color online) Experimental data (scatter plots) and model predictions (solid curves) at 330 mW, 440 mW, and 550 mW excitation powers for (A) methanol and (B) ethanol.

or incorporating this into the software routine for real-time measurements; however, this was not necessary for the goals of the current study.

4. Discussion and Conclusion

Methanol and ethanol were chosen for the current study due to their immediate availability, ease of finding the necessary photothermal parameters, and the availability of results from previous experimental methods yielding absorption coefficients for comparison. We have measured absorption coefficients of $(3.6 \pm 0.3) \times 10^{-4}\,\mathrm{cm}^{-1}$ and $(2.4 \pm 0.2) \times 10^{-4}\,\mathrm{cm}^{-1}$ for methanol and ethanol, respectively. Previously, these values had been measured using the traditional "pinhole" method mentioned above as $(5.9 \pm 0.5) \times 10^{-4}\,\mathrm{cm}^{-1}$ and $(6.8 \pm 0.5) \times 10^{-4}\,\mathrm{cm}^{-1}$ for methanol and ethanol, respectively [2]. We have measured the values with improved precision, but what is more noteworthy is the difference in relative absorption coefficient between these two liquids. By imaging the phase profiles directly with digital holography, this relation is straightforward and unmistakable, suggesting much improved accuracy over the traditional method.

Noise levels of our system were determined between each measurement by imaging the sample with no excitation beam present and taking the standard deviation of this phase profile to indicate background noise. Values ranged between 0.03 and 0.17 rad, with 0.12 rad being typical. This equates to the typical absorption coefficient measurement tolerance indicated above for the current experimental parameters. In addition to the determination of absorption coefficient, the phase shift caused by a thermal lens has a direct mathematical relationship with shifts in optical path length, index of refraction, and temperature of the media. As such, a direct measurement of the phase shift will yield this data as well with relative precision. Using the current typical noise level of our system and the relation from Eq. (3), the average change in temperature has been measured to a precision 0.0072 K. The refractive index has been measured to 2.4×10^{-6} precision. Additionally, the optical path length difference has been resolved to 12 nm resolution. It is expected that, with careful isolation and construction, future apparatus could improve the current precision by up to an order of magnitude without compromising speed or compactness.

We have successfully shown the usefulness of our method to obtain characteristic photothermal properties of pure substances, but thermal lens spectroscopy (TLS) and absorption spectroscopy are also very sensitive to sample contamination or other analytes [12,13]. In fact, TLS has been shown to have detection levels several orders of magnitude better than conventional spectrophotometric techniques [14]. With the improvements of the current study, TLS by digital holography could become a widely-used ultrasensitive tool for many analytical chemistry applications.

In addition to its usefulness in chemical analysis, thorough testing and understanding of the thermal lens effect can be important in the observation of optical effects. Of particular near-term interest to us is the nanometric measurement of optical radiation pressure deformation from photon momentum exchange across a fluid interface. This effect will also result in a phase shift measurable by digital holography; however, it is very weak and would be

dominated by the thermal lens effect. For this reason, we will test the time-resolved regime of the model by imaging at shortened time scales. This will be done to test the completeness of the model as well as to reduce the thermal effect on the media to a level where weaker optical phenomenon can be observed without the dominating effect of thermal lensing present. Additionally, the thermal time constant, τ, increases with the square of the excitation beam radius. Increasing this radius will drastically increase the time scale of thermal effects. Initial simulations and studies suggest that decoupling the two effects and imaging with digital holography should prove successful for fluid-fluid interfaces as outlined in [11].

This work is supported in part by the National Science Foundation (NSF), grant 0755705.

References

1. A. Marcano, C. Loper, and N. Melikechi, "High sensitivity absorption measurement in water and glass samples using a mode-mismatched pump-probe lens method," Appl. Phys. Lett. **78**, 3415–3417 (2001).
2. H. Cabrera, A. Marcano, and Y. Castellanos, "Absorption coefficient of nearly transparent liquids measured using thermal lens spectrometry," Condens. Matter Phys. **9**, 385–389 (2006).
3. J. Shen, R. D. Lowe, and R. D. Snook, "A model for cw laser induced mode-mismatched dual-beam thermal lens spectrometry," Chem. Phys. **165**, 385–396 (1992).
4. J. Shen, M. L. Baesso, and R. D. Snook, "Three-dimensional model for cw laser-induced mode-mismatched dual-beam thermal lens spectrometry and time-resolved measurements of thin-film samples," J. Appl. Phys. **75**, 3738–3748 (1994).
5. J. Shen, A. J. Soroka, and R. D. Snook, "A model for cw laser induced mode-mismatched dual-beam thermal lens spectrometry based on probe beam profile image detection," J. Appl. Phys. **78**, 700–708 (1995).
6. S. E. Bialkowski, *Photothermal Spectroscopy Methods for Chemical Analysis* (Wiley, 1996).
7. E. Cuche, F. Bevilacqua, and C. Depeursinge, "Digital holography for quantitative phase-contrast imaging," Opt. Lett. **24**, 291–293 (1999).
8. C. J. Mann, L. Yu, C.-M. Lo, and M. K. Kim, "High-resolution quantitative phase-contrast microscopy by digital holography," Opt. Express **13**, 8693–8698 (2005).
9. S. D. Woodruff and E. S. Yeung, "Refractive index and absorption detector for liquid chromatography based on Fabry–Perot interferometry," Anal. Chem. **54**, 1174–1178 (1982).
10. L. Yu and M. K. Kim, "Wavelength-scanning digital interference holography for tomographic 3D imaging using the angular spectrum method," Opt. Lett. **30**, 2092–2094 (2005).
11. D. C. Clark and M. K. Kim, "Nanometric measurement of optical pressure deformation of fluid interface by digital holography," Proc. SPIE **7908**, 79080T (2011).
12. W. S. Pegau, D. Gray, and J. R. V. Zaneveld, "Absorption and attenuation of visible and near-infrared light in water: dependence on temperature and salinity," Appl. Opt. **36**, 6035–6046 (1997).
13. M. Babin, D. Stramski, G. M. Ferrari, H. Claustre, A. Bricaud, G. Obolensky, and N. Hoepffner, "Variations in the light absorption coefficients of phytoplankton, nonalgal particles, and dissolved organic matter in coastal waters around Europe," J. Geophys. Res. **108**, 3211 (2003).
14. S. M. Colcombe, R. D. Lowe, and R. D. Snook, "Thermal lens investigation of the temperature dependence of the refractive index of aqueous electrolyte solutions," Anal. Chim. Acta **356**, 277–288 (1997).